J|A|C|S
ARTICLES
Published on Web 09/13/2006

# Control Over Charge Separation in Phthalocyanine−Anthraquinone Conjugates as a Function of the Aggregation Status

Andreas Gouloumis,[†,‡] David González-Rodríguez,[†] Purificación Vázquez,[†] Tomás Torres,*[,†] Shenggao Liu,[§,||] Luis Echegoyen,*[,§] Jeff Ramey,[⊥] Gordon L. Hug,[#] and Dirk M. Guldi*[,⊥]

*Contribution from the Departamento de Química Orgánica, Facultad de Ciencias, Universidad Autónoma de Madrid, E-28049 Madrid, Spain, Departamento de Química Orgánica, Facultad de Ciencias Químicas, Universidad Complutense de Madrid, E-28040 Madrid, Spain, Department of Chemistry, Clemson University, Clemson, South Carolina 29634, Radiation Laboratory, University of Notre Dame, South Bend, Indiana 46556, and Institute of Physical Chemistry, University of Erlangen, 91058 Erlangen, Germany*

Received August 5, 2005; E-mail: tomas.torres@uam.es; luis@clemson.edu; dirk.guldi@chemie.uni-erlangen.de

***Abstract:*** We have prepared three isomeric donor−acceptor systems, in which two phthalocyanine (Pc) units have been attached to the 1-,5- (**1a**), 1-,8- (**1b**), or 2-,6- (**1c**) positions of a central anthraquinone (AQ) moiety, leading to packed (**1b**) or extended (**1a** and **1c**) topologies. The electronic interactions between the donor and the acceptor in the ground state or in the excited states have been studied by different electrochemical and photophysical techniques. Due to the markedly different topologies, we have been able to modify these interactions at the intramolecular level and, by a proper choice of the solvent environment, at the intermolecular level within aggregates. In triad **1b**, the ZnPc units are forced to $\pi$-stack cofacially and out of the plane of the AQ ring. Consequently, this molecule shows strong inter-Pc interactions that give rise to intramolecular excitonic coupling but a relatively small electronic communication with the AQ acceptor through the vinyl spacers. On the contrary, the 1-,5- or 2-,6-connections of triads **1a** and **1c** allow for an efficient $\pi$-conjugation between the active units that extends over the entire planar system. These two molecules tend to aggregate in aromatic solvents by $\pi-\pi$ stacking, giving rise to J-type oligomers. Photoexcitation of the Pc units of **1a**−**c** results in the formation of the $Pc^{\bullet+}-AQ^{\bullet-}$ charge transfer state. We have demonstrated that the kinetics of these electron transfer reactions is greatly dependent on the aggregation status of the triads.

## Introduction

In the last two decades great efforts have been spent in the study and understanding of the factors that influence photoinduced electron-transfer reactions in model molecular systems, comprised of electron-donor and acceptor chromophores linked by well-defined spacers.[1] This area of research is continuously providing evidence for the effect of the nature of the donor and acceptor components,[2a] their relative distance,[2b−e] orientation,[2f,g] or electronic coupling[2h−l] (mediated by the spacer), or of solvent polarity,[2m−o] on the yield and kinetics of charge transfer. While the knowledge gathered enables researchers to design discrete molecular systems with enhanced charge-separation performances, its projection to solid-state systems for photovoltaic applications,[3] where other factors come into play due to strong intermolecular interactions, represents a further challenge.

[†] Universidad Autónoma de Madrid.
[‡] Universidad Complutense de Madrid.
[§] Clemson University.
[||] Current address: ChevronTexaco Energy Technology Co., Richmond, CA 94802.
[⊥] University of Erlangen.
[#] University of Notre Dame.

(1) (a) Balzani, V.; Scandola, F. *Supramolecular Photochemistry*; Ellis Horwood: Chichester, U.K., 1991; pp 161−196, 355−394. (b) *Electron Transfer in Chemistry, Vol. I*−*V*; Balzani, V., Ed.; Wiley-VCH: Weinheim, 2001.

(2) For some representative examples, see: (a) Imahori, H.; Yamada, H.; Guldi, D. M.; Endo, Y.; Shimomura, A.; Kundu, S.; Yamada, K.; Okada, T.; Sakata, Y.; Fukuzumi, S. *Angew. Chem., Int. Ed.* **2002**, *41*, 2344−2347. (b) Jordan, K. D.; Paddon-Row, M. N. *Chem. Rev.* **1992**, *92*, 395−410. (c) Lewis, F. D.; Letsinger, R. L.; Wasielewski, M. R. *Acc. Chem. Res.* **2001**, *34*, 159−170. (d) Smitha, M. A.; Prasad, E.; Gopidas, K. R. *J. Am. Chem. Soc.* **2001**, *123*, 1159−1165. (e) Masahiko, S.; Satoshi, H.; Kusano, H.; Kuragaki, M.; Makino, M.; Sasaki, H.; Smith, T. A.; Ghiggino, K. P. *J. Phys. Chem. B* **2001**, *105*, 10407−10415. (f) Guldi, D. M.; Luo, C.; Prato, M.; Troisi, A.; Zerbetto, F.; Scheloske, M.; Dietel, E.; Bauer, W.; Hirsch, A. *J. Am. Chem. Soc.* **2001**, *123*, 9166−9167. (g) Guldi, D. M.; Hirsch, A.; Scheloske, M.; Dietel, E.; Troisi, A.; Zerbetto, F.; Prato, M. *Chem.*−*Eur. J.* **2003**, *9*, 4968−4979. (h) Guldi, D. M.; Maggini, M.; Scorrano, G.; Prato, M. *J. Am. Chem. Soc.* **1997**, *119*, 8363. (i) Gust, D.; Moore, T. A.; Moore, A. L.; Devadoss, C.; Liddell, P. A.; Hermant, R.; Nieman, R. A.; Demanche, L. J.; DeGraziano, J. M.; Gouni, I. *J. Am. Chem. Soc.* **1992**, *114*, 3590−3603. (j) Imahori, H.; Hagiwara, K.; Aoki, M.; Akiyama, T.; Taniguchi, S.; Okada, T.; Shirakawa, M.; Sakata, Y. *J. Am. Chem. Soc.* **1996**, *118*, 11771−11782. (k) Tsue, H.; Imahori, H.; Kaneda, T.; Tanaka, Y.; Okada, T.; Tamaki, K.; Sakata, Y. *J. Am. Chem. Soc.* **2000**, *122*, 2279−2288. (l) Kilsa, K.; Kajanus, J.; Macpherson, A. N.; Martensson, J.; Albinsson, B. *J. Am. Chem. Soc.* **2001**, *123*, 3069−3080. (m) Lokan, N. R.; Paddon-Row, M. N.; Koeberg, M.; Verhoeven, J. W. *J. Am. Chem. Soc.* **2000**, *122*, 5075−5081. (n) Imahori, H.; El-Khouly, M. E.; Fujitsuka, M.; Ito, O.; Sakata, Y.; Fukuzumi, S. *J. Phys. Chem. A* **2001**, *105*, 325−332. (o) Fujitsuka, M.; Tsuboya, N.; Hamasaki, R.; Ito, M.; Onodera, S.; Ito, O.; Yamamoto, Y. *J. Phys. Chem. A* **2003**, *107*, 1452−1458.


**10.1021/ja055344+ CCC: $33.50** 

Organic solar cells in which the active layer consists of donor−acceptor ensembles have been proposed as one of the most promising,[4] due to the large interfacial area between the donor and acceptor moieties and the possibility of controlling the nanoscopic morphology through supramolecular self-assembly, in a biomimetic fashion.[5] Since most of these photoactive units are planar $\pi$-conjugated systems, much interest has been recently devoted to their noncovalent organization by $\pi-\pi$ stacking and to the study of the electronic interactions between the donor and acceptor components, both within and between the molecules in the stacks.[5,6]

Among these photoactive units, phthalocyanines (Pcs) and related systems[7] play a central role in view of their outstanding electronic properties, which rely on their extensive aromatic $\pi$-system. These planar macrocycles are ideally suited for photovoltaic applications[8] since they present exceptional optical and thermal stability and strong absorption in the visible, finely tunable redox properties and may be incorporated into different kinds of condensed phases, due to their tendency to aggregate by $\pi-\pi$ stacking. In this regard, we and others have recently prepared different systems in which Pcs or analogues are covalently attached to other electro- or photoactive units, such as ruthenium−bipyridine complexes,[9] TTF derivatives,[10] fullerene,[11] porphyrins,[12] or ferrocene,[13] in order to study their electronic interactions in the ground, charged, or excited state. On the other hand, while a considerable amount of work has been published on the properties of porphyrin−quinone dyads, designed to reproduce the primary processes in natural photosynthesis,[14] only a handful have involved Pc−anthraquinone (AQ) ensembles.[15] The usual mechanism that operates in these systems involves photoexcitation of the macrocycle to yield the singlet excited state, from which electron transfer to the electronically poor quinone derivative takes place.

In this general context, we present herein the synthesis and the electrochemical and photophysical properties of a series of three isomeric Pc−AQ−Pc triads (**1a**−**c**), covalently linked by ethenyl spacers (Figure 1). The three isomers only differ in the connecting positions of the Pc units to the central AQ moiety (i.e., 1-,5-; 1-,8-; or 2-,6-), which leads to distinct relative topological configurations of the Pcs. Whereas **1a** and **1c**[15d] are presumed to adopt an all-planar $\pi$-extended conformation, the 1-,8- connection in triad **1b** would force the two Pcs to be cofacially stacked and out of the plane of the AQ $\pi$-system.[6a,13a,16,17] Consequently, we anticipate quite different interchromophoric electronic interactions for these two kinds of arrangements, both at the intramolecular (via the extended $\pi$-surface) and the intermolecular level (via $\pi-\pi$ stacking). We demonstrate in this article the effect of the aggregation status of triads **1a**−**c**, as a function of molecular topology and solvent environment, on their redox and photoinduced charge-separation properties.


(3) (a) Brabec, C.; Sariciftci, N. S.; Hummelen, J. C. *Adv. Funct. Mater.* **2001**, *11*, 15−26. (b) Winder, C.; Sariciftci, N. S. *J. Mater. Chem.* **2004**, *14*, 1077−1086.

(4) (a) Eckert, J. F.; Nicoud, J. F.; Nierengarten, J. F.; Liu, S. G.; Echegoyen, L.; Barigelletti, F.; Armaroli, N.; Ouali, L.; Krasnikov, V.; Hadziioannou, G. *J. Am. Chem. Soc.* **2000**, *122*, 7467−7479. (b) Peeters, E.; Hal, P. A. V.; Knol, J.; Brabec, C. J.; Sariciftci, N. S.; Hummelen, J. C.; Janssen, R. A. J. *J. Phys. Chem. B* **2000**, *104*, 10174−10190. (c) Wang, L. H.; Chen, Z. K.; Xiao, Y.; Kang, E. T.; Huang, W. *Macromol. Rapid Commun.* **2000**, *21*, 897−900. (d) El-ghayoury, A.; Schenning, A. P. H. J.; van Hal, P. A.; van Duren, J. K. J.; Janssen, R. A. J. *Angew. Chem., Int. Ed.* **2001**, *40*, 3660−3663. (e) Pourtois, G.; Beljonne, D.; Cornil, J.; Ratner, M. A.; Brédas, J. L. *J. Am. Chem. Soc.* **2002**, *124*, 4436−4447. (f) Cravino, A.; Saricifti, N. S. *J. Mater. Chem.* **2002**, *12*, 1931−1943.

(5) (a) Würthner, F.; Thalacker, C.; Sautter, A. *Adv. Mater.* **1999**, *11*, 754−758. (b) El-ghayoury, A.; Peeters, E.; Schenning, A. P. H. J.; Meijer, E. W. *Chem. Commun.* **2000**, 1969−1970. (c) Schmidt-Mende, L.; Fechtenkötter, A.; Müllen, K.; Moons, E.; Friend, R. H.; Mackenzie, J. D. *Science* **2001**, *293*, 1119−1122. (d) Syamakumari, A.; Schenning, A. P. H. J.; Meijer, E. W. *Chem.—Eur. J.* **2002**, *8*, 3353−3361. (e) Samori, P.; Yin, X.; Tchebotareva, N.; Wang, Z.; Pakula, T.; Jäckel, F.; Watson, M. D.; Venturini, A.; Müllen, K.; Rabe, J. P. *J. Am. Chem. Soc.* **2004**, *126*, 3567−3575.

(6) (a) Giaimo, J. M.; Gusev, A. V.; Wasielewski, M. R. *J. Am. Chem. Soc.* **2002**, *124*, 8530−8531. (b) van der Boom, T.; Hayes, R. T.; Zhao, Y.; Bushard, P. J.; Weiss, E. A.; Wasielewski, M. R. *J. Am. Chem. Soc.* **2002**, *124*, 9582−9590. (c) Rybtchinski, B.; Sinks, L. E.; Wasielewski, M. R. *J. Phys. Chem. A* **2004**, *108*, 7497−7505. (d) Ahrens, M. J.; Sinks, L. E.; Rybtchinski, B.; Liu, W.; Jones, B. A.; Giaimo, J. M.; Gusev, A. V.; Goshe, A. J.; Tiede, D. M.; Wasielewski, M. R. *J. Am. Chem. Soc.* **2004**, *126*, 8284−8294. (e) Marcos Ramos, A.; Meskers, S. C. J.; Beckers, E. H. A.; Prince, R. B.; Brunsveld, L.; Janssen, R. A. J. *J. Am. Chem. Soc.* **2004**, *126*, 9630−9644. (f) Würthner, F.; Chen, Z.; Hoeben, F. J. M.; Osswald, P.; You, C.-C.; Jonkheijm, P.; Herrikhuyzen, J. V.; Schenning, A. P. H. J.; van der Schoot, P. P. A. M.; Meijer, E. W.; Beckers, E. H. A.; Meskers, S. C. J.; Janssen, R. A. J. *J. Am. Chem. Soc.* **2004**, *126*, 10611−10618. (g) Li, X.; Sinks, L. E.; Rybtchinski, B.; Wasielewski, M. R. *J. Am. Chem. Soc.* **2004**, *126*, 10810−10811. (h) Rybtchinski, B.; Sinks, L. E.; Wasielewski, M. R. *J. Am. Chem. Soc.* **2004**, *126*, 12268−12269. (i) Beckers, E. H. A.; Meskers, S. C. J.; Schenning, A. P. H. J.; Chen, Z.; Würthner, F.; Marsal, P.; Beljonne, D.; Cornil, J.; Janssen, R. A. J. *J. Am. Chem. Soc.* **2006**, *128*, 649−657.

(7) (a) de la Torre, G.; Vázquez, P.; Agulló-López, F.; Torres, T. *J. Mater. Chem.* **1998**, *8*, 1671−1683. (b) del Rey, B.; Keller, U.; Torres, T.; Rojo, G.; Agulló-López, F.; Nonell, S.; Marti, C.; Brasselet, S.; Ledoux, I.; Zyss, J. *J. Am. Chem. Soc.* **1998**, *120*, 12808−12817. (c) Claessens, C. G.; González-Rodríguez, D.; Torres, T. *Chem. Rev.* **2002**, *102*, 835−853. (d) *The Porphyrin Handbook*; Kadish, K. M., Smith, K. M., Guillard, R., Eds.; Academic Press: San Diego, CA, 2003; Vols. 15−20. (e) de la Torre, G.; Vázquez, P.; Agulló-López, F.; Torres, T. *Chem. Rev.* **2004**, *104*, 3723−3750. (f) González-Rodríguez, D.; Torres, T.; Herranz, M. A.; Rivera, J.; Echegoyen, L.; Guldi, D. M. *J. Am. Chem. Soc.* **2004**, *126*, 6301−6313. (g) Torres, T. *Angew. Chem., Int. Ed.* **2006**, *45*, 2834−2837; *Angew. Chem.* **2006**, *118*, 2900−2903.

(8) (a) He, J.; Benkö, G.; Korodi, F.; Polívka, T.; Lomoth, R.; Akermark, B.; Sun, L.; Hagfeldt, A.; Sundström, V. *J. Am. Chem. Soc.* **2002**, *124*, 4922. (b) Loi, M. A.; Denk, P.; Hoppe, H.; Neugebauer, H.; Winder, C.; Meissner, D.; Brabec, C. J.; Sariciftci, N. S.; Gouloumis, A.; Vázquez, P.; Torres, T. *J. Mater. Chem.* **2003**, *13*, 700−704. (c) Loi, M. A.; Denk, P.; Hoppe, H.; Neugebauer, H.; Meissner, D.; Winder, C.; Brabec, C. J.; Sariciftci, N. S.; Gouloumis, A.; Vázquez, P.; Torres, T. *Synth. Met.* **2003**, *137*, 1491−1492.

(9) González, A.; Vázquez, P.; Torres, T.; Guldi, D. M. *J. Org. Chem.* **2003**, *68*, 8635−8642.

(10) Farren, C.; Christensen, C. A.; FitzGerald, S.; Bryce, M. R.; Beeby, A. *J. Org. Chem.* **2002**, *67*, 9130−9139.

(11) (a) Gouloumis, A.; Liu, S.-G.; Sastre, A.; Vázquez, P.; Echegoyen, L.; Torres, T. *Chem.—Eur. J.* **2000**, *6*, 3600−3607. (b) González-Rodríguez, D.; Torres, T. In *The Exciting World of Nanocages and Nanotubes*; Kamat, P., Guldi, D. M., Kadish, K., Eds.; Proceeding of the Electrochemical Society, Fullerenes; ECS: Pennington, NJ, 2002; Vol. 12, pp 195−210. (c) Guldi, D. M.; Zilbermann, I.; Gouloumis, A.; Vázquez, P.; Torres, T. *J. Phys. Chem. B* **2004**, *108*, 18485−18494. (d) Guldi, D. M.; Gouloumis, A.; Vázquez, P.; Torres, T.; Georgakilas, V.; Prato, M. *J. Am. Chem. Soc.* **2005**, *127*, 5811−5813. (e) de la Escosura, A.; Martínez-Díaz, M. V.; Guldi, D. M.; Torres, T. *J. Am. Chem. Soc.* **2006**, *128*, 4112−4118.

(12) (a) Ambroise, A.; Wagner, R. W.; Rao, P. D.; Riggs, J. A.; Hascoat, P.; Diers, J. R.; Seth, J.; Lammi, R. K.; Bocian, D. F.; Holten, D.; Lindsey, J. S. *Chem. Mater.* **2001**, *13*, 1023−1034. (b) Tomé, J. P. C.; Pereira, A. M. V. M.; Alonso, C. M. A.; Neves, M. G. P. M. S.; Tomé, A. C.; Silva, A. M. S.; Cavaleiro, J. A. S.; Martínez-Díaz, M. V.; Torres, T.; Guldi, D. M.; Rahman, G. M. A.; Ramey, J. *Eur. J. Org. Chem.* **2006**, 257−267.

(13) (a) González, A.; Vázquez, P.; Torres, T. *Tetrahedron Lett.* **1999**, *40*, 3263−3266. (b) González, A.; Claessens, C. G.; Martín, G.; Ledoux, I.; Vázquez, P.; Zyss, J.; Agulló-López, F.; Torres, T. *Synth. Met.* **2003**, *137*, 1487−1488.

(14) (a) Wasielewski, M. R. *Chem. Rev.* **1992**, *34*, 435−461. (b) Gust, D.; Moore, T. A.; Moore, A. L. *Acc. Chem. Res.* **1993**, *26*, 198−205. (c) Kurreck, H.; Huber, M. *Angew. Chem., Int. Ed. Engl.* **1995**, *34*, 849−866. (d) Gust, D.; Moore, T. A.; Moore, A. L. *Acc. Chem. Res.* **2001**, *34*, 40−48. (e) Huber, M. *Eur. J. Org. Chem.* **2001**, *23*, 4379−4389.

(15) (a) Li, L.; Shen, S.; Yu, Q.; Zhou, Q.; Xu, H. *J. Chem. Soc., Chem. Commun.* **1991**, 619−620. (b) Kobayashi, N.; Ohya, T.; Sato, M.; Nakajima, S. *Inorg. Chem.* **1993**, *32*, 1803−1808. (c) Li, X.; Ng, D. K. P. *Tetrahedron Lett.* **2001**, *42*, 305−309. (d) Gouloumis, A.; Liu, S.-G.; Vázquez, P.; Echegoyen, L.; Torres, T. *Chem. Commun.* **2001**, 399−400.

(16) Some excited-state properties of cofacial bisporphyrins have been studied: (a) Bolze, F.; Gros, C. P.; Harvey, P. D.; Guilard, R. *J. Porphyrins Phthalocyanines* **2001**, *5*, 569−574. (b) Loh, Z.-H.; Miller, S. E.; Chang, C. J.; Carpenter, S. D.; Nocera, D. G. *J. Phys. Chem. A* **2002**, *106*, 11700−11708.

(17) Similar 1,8-naphthalene- or 1,8-anthracene-linked bisphthalocyanines have been reported: (a) Leznoff, C. C.; Lam, H.; Nevin, W. A.; Kobayashi, N.; Janda, P.; Lever, A. B. P. *Angew. Chem., Int. Engl.* **1987**, *26*, 1021−1023. (b) Lam, H.; Marcuccio, S. M.; Svirskaya, P. I.; Greenberg, S.; Lever, A. B. P.; Leznoff, C. C.; Cerny, R. L. *Can. J. Chem.* **1989**, *67*, 1087−1097. (c) Kobayashi, N.; Yanagisawa, Y.; Osa, T.; Lam, H.; Leznoff, C. C. *Anal. Chem.* **1990**, *6*, 813−817. (d) Kobayashi, N.; Lam, H.; Nevin, W. A.; Janda, P.; Leznoff, C. C.; Lever, A. B. P. *Inorg. Chem.* **1990**, *29*, 3415−3425.

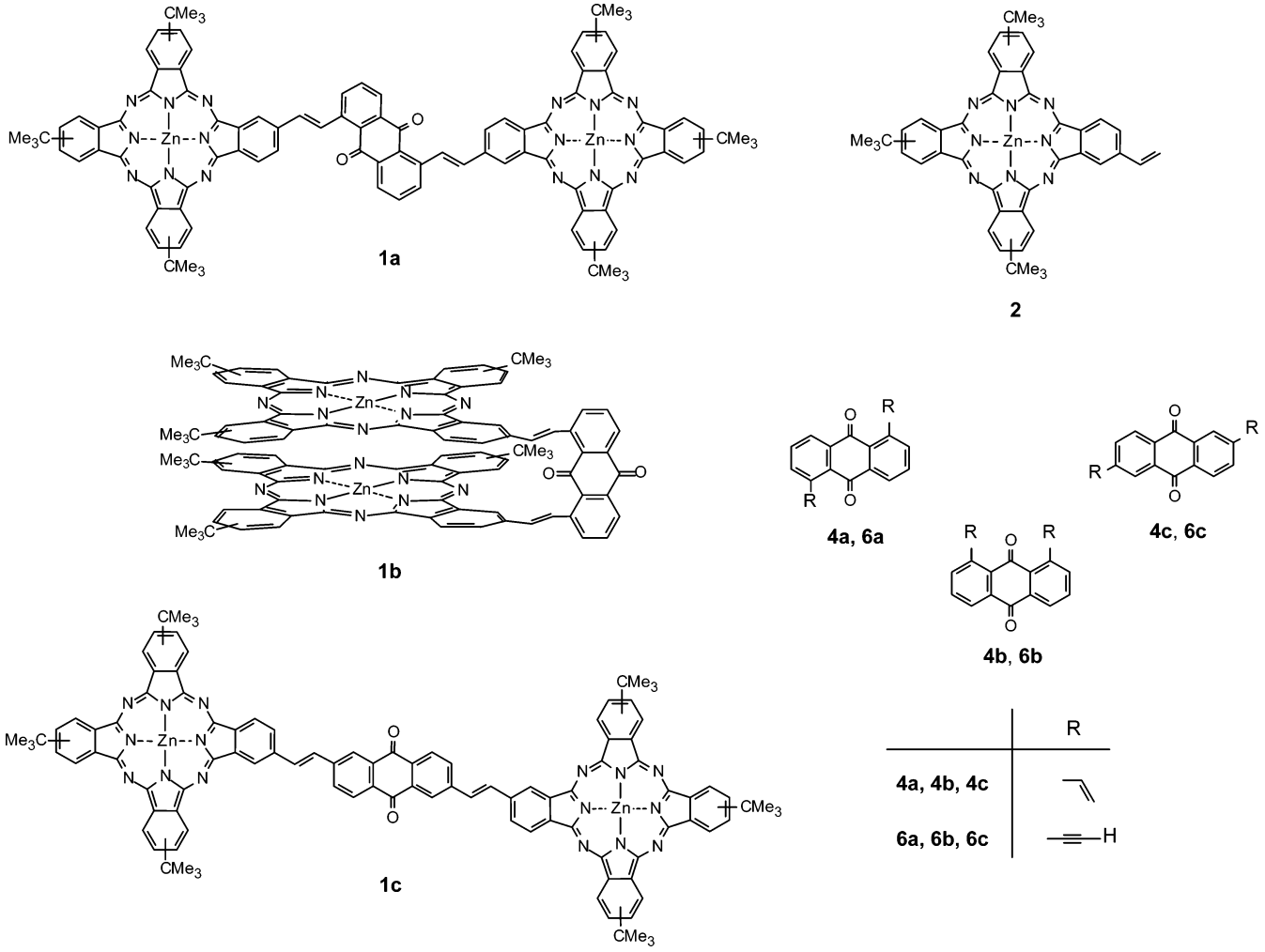


***Figure 1.*** Pc−AQ−Pc triads **1a**−**c** and reference compounds Pc **2**, vinylanthraquinones **4a**−**c**, and ethynylanthraquinones **6a**−**c**.

## Results and Discussion

**Synthesis.** The synthesis of the Pc−AQ−Pc systems **1a**−**c** was carried out by a Heck-type coupling reaction between tri-*tert*-butyl-vinylphthalocyaninatozinc(II) (**2**)[15d,18] and the corresponding diiodoanthraquinone **3a**−**c**,[19] as depicted in Scheme 1. Among the different palladium catalysts tested, $(MeCN)_2PdCl_2$ afforded the best yields (70−75%).

As reference AQ compounds, the diethenyl- and diethynyl-derivatives **4a**, **4b**,[20] and **4c** and **6a**, **6b**, and **6c**[21] were prepared from **3a**−**c** employing palladium-catalyzed Stille[22] or Sonogashira[23] methodologies, respectively. Thus, the reaction of the corresponding diiodoanthraquinone **3a**−**c** with tributyl(vinyl)-tin in the presence of $Pd(PPh_3)_4$ yielded **4a**−**c** in 77−89%. On the other hand, the synthesis of **6a**−**c** required two steps from **3a**−**c** that proceeded in 60−72% overall yield: a $(PPh_3)_2PdCl_2$-catalyzed coupling with trimethylsilylacetylene, affording **5a**−**c**, and fluoride-mediated cleavage of the protecting groups.

Triads **1a** and **1c** are barely soluble in aromatic solvents such as toluene or *o*-dichlorobenzene (*o*-DCB) but very soluble in THF, 1,4-dioxane, or pyridine. Isomer **1b** is an exception, being also quite soluble in aromatic solvents. Due to their tendency to aggregate in solution (see below) and the existence of several positional isomers, the $^1$H NMR spectra of **1a**−**c** presented very broad features for the aromatic protons. In addition, a broad signal from the protons of the *tert*-butyl groups could be seen in the range 2.1−1.8 ppm for the three triads. MALDI-TOF MS experiments revealed the molecular ion of **1a**−**c** as the most prominent peak (at $m/z$ = 1744−1753), displaying an isotopic pattern that is identical for the three triads and that compares properly with the simulated one.

**Ground State. A. Electronic Absorption Spectra. Study of the Aggregation Status of 1a−c in Different Solvents.** The absorption spectra of **1a**−**c** in THF (Figure 2a), although resembling the component spectra (i.e., 9,10-anthraquinone and ZnPc), show a marked deviation from a simple superposition. Most eminently, the maximum of the ZnPc *Q*-band of **1a** and **1c** reveals a notable red-shift and splitting with respect to model compound **2**, thus reflecting the coupling of the ZnPc chromophore, mediated through the linker, to the AQ moiety.

(18) Compound **2** was used as a statistical mixture of regioisomers that could not be separated by chromatography. See: Gürlach, B.; Dachtler, M.; Glaser, T.; Albert, K.; Hanack, M. *Chem.—Eur. J.* **2001**, *29*, 2459−2465.
(19) (a) House, H.; Koepsell, D.; Campbell, W. *J. Org. Chem.* **1972**, *37*, 1003−1011. (b) Kendall, J. K.; Shechter, H. *J. Org. Chem.* **2001**, *66*, 6643−6649.
(20) For other methods of preparation, see: (a) Manecke, G.; Kretzschmar, H. J. *Macromol. Chem.* **1973**, *169*, 15−35. (b) Tamayo, N.; Echavarren, A. M.; Paredes, M. C.; Fariña, F.; Noheda, P. *Tetrahedron Lett.* **1990**, *36*, 5189−5192.
(21) For other methods of preparation, see: Murty, K. V. S. N.; Vasella, A. *Helv. Chim. Acta* **2001**, *84*, 939−963.
(22) Stille, J. K. *Angew. Chem., Int. Ed. Engl.* **1986**, *25*, 505−519.
(23) Sonoghasira, K.; Tohda, Y.; Hagihara, N. *Tetrahedron Lett.* **1975**, *21*, 4467−4470.

***Scheme 1.*** Synthesis of Pc−AQ−Pc Triads **1a**−**c**, Vinylanthraquinones **4a**−**c**, Trimethylsilylethynylanthraquinones **5a**−**c**, and Ethynylanthraquinones **6a**−**c**[a]

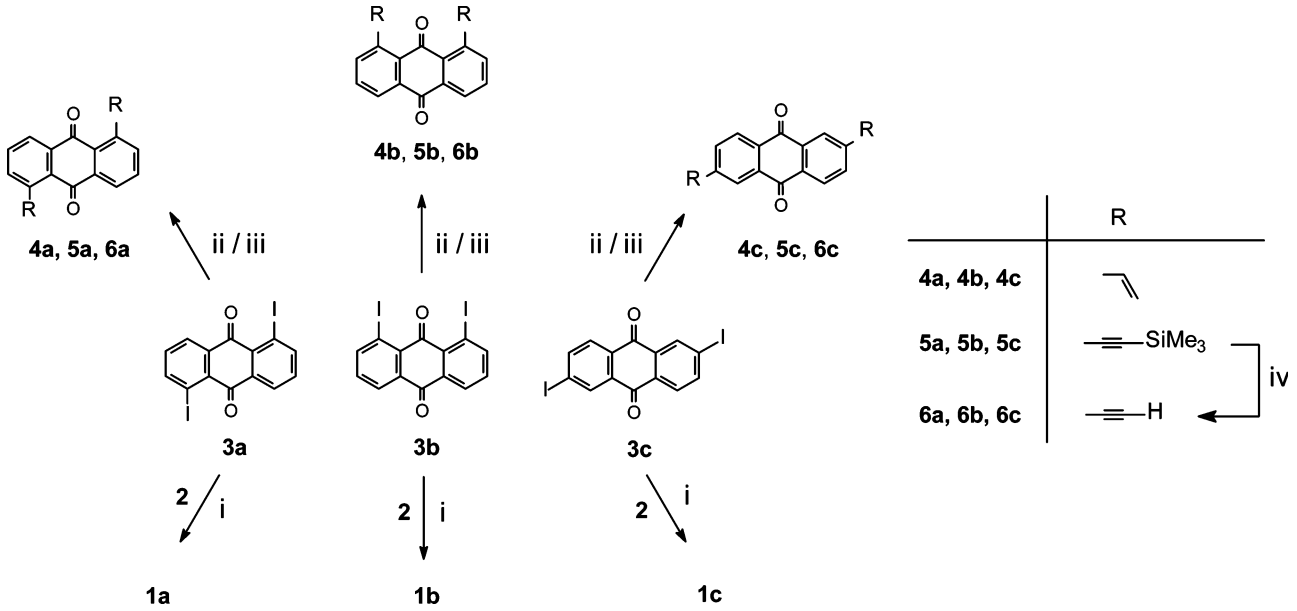


[a] (i) $(MeCN)_2PdCl_2$, $Bu_4NBr$, $Et_3N$, toluene, 100 °C; (ii) tributyl(vinyl)tin, $Pd(PPh_3)_4$, toluene, 100 °C (for **4a**−**c**); (iii) trimethylsilylacetylene, $Pd(PPh_3)_4$, CuI, $Et_3N$, toluene, 100 °C (for **5a**−**c**); (iv) $Bu_4NF$, $CHCl_3$, 60 °C.

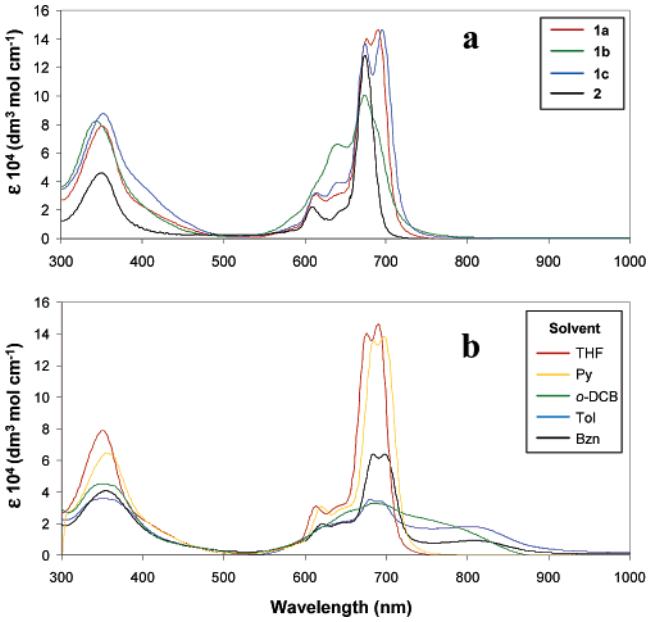


***Figure 2.*** (a) Ground-state absorption spectra of **2** and **1a**−**c** ($c$ = ca. $10^{-6}$ M) in THF. (b) Absorption spectra of **1a** in different solvents ($c$ = ca. $10^{-5}$ M).

The order $\lambda_{max}$(**1a**) < $\lambda_{max}$(**1c**) is coherent for a higher degree of electronic coupling for the beta versus the alpha substitution pattern. On the contrary, in **1b**, a substantial broadening and a new band toward the blue of the *Q*-band maximum is observed. The imposed cofacial arrangement of the Pc macrocycles, which avoids for an efficient $\pi$-conjugation with the AQ moiety and leads to intramolecular excitonic coupling between the two stacked ZnPcs is, most likely, responsible for these effects.[17]

When testing different solvents (Figure 2b), the shapes of the absorption spectra of **1a** and **1c** reveal significant changes that account for the aforementioned solubility properties of these molecules. Whereas THF or pyridine solutions at concentrations between $10^{-4}$ and $10^{-7}$ M afford absorption spectra that are typical of monomeric species (see Figures S1−S4), benzonitrile, *o*-DCB, or toluene solutions of **1a** and **1c** display a substantial broadening of the Pc *Q*-band, which is indicative of intermolecular aggregation phenomena induced by the aromatic solvent.[24] Solvents such as THF or pyridine seem to be able to disrupt $\pi-\pi$ stacking by coordination to the metal center. In this context, **1b** is an important reference, since it shows very similar spectra in all solvents and at different concentrations ($10^{-5}$−$10^{-7}$ M; see Figures S5 and S6). This indicates a lower tendency to form intermolecular aggregates due to its molecularly enforced packed structure. Pc compound **2** also presents a broadening of the *Q*-band, but this is only significant at quite high concentrations (>$10^{-5}$ M) in toluene (see, for instance, Figures S7 and S8) or *o*-DCB.

In particular, the absorption spectra of **1a** and **1c** in benzonitrile shows two clear bands in the region 600−900 nm at concentrations of $10^{-4}$−$10^{-6}$ M: the monomeric ZnPc *Q*-band and a second broader absorption band (centered at 810 nm for **1a**; see Figure 2b).[25] The latter band was ascribed to supramolecularly stacked oligomeric species, since the extinction coefficient of the monomeric ZnPc absorption increases at the expense of this new band (i) upon dilution (Figure 3a) and (ii) upon addition of pyridine (Figure 3b). No further spectral change was appreciated at very dilute solutions (< $5 \times 10^{-7}$ M) or after the addition of ca. 20 equiv of pyridine, suggesting that only monomeric species are present. Given the well-defined shape of the absorption bands and the presence of clear isosbestic points in the spectra of **1a** (665 and 720 nm) or **1c** (668 and 729 nm; see Figures S9 and S10) in benzonitrile, we presume that a dynamic equilibrium between monomers and dimers is taking place at this concentration range, though the presence of small oligomers should not be discarded. This hypothesis is

(24) Snow, A. W. In *The Porphyrin Handbook*; Kadish, K. M., Smith, K. M., Guillard, R., Eds.; Academic Press: San Diego, CA, 2003; Vol. 17, pp 129−176.
(25) In the case of compound **1c** the maximum of the dimer band overlaps the red edge of the monomer absorption band (see Figures S9 and S10).

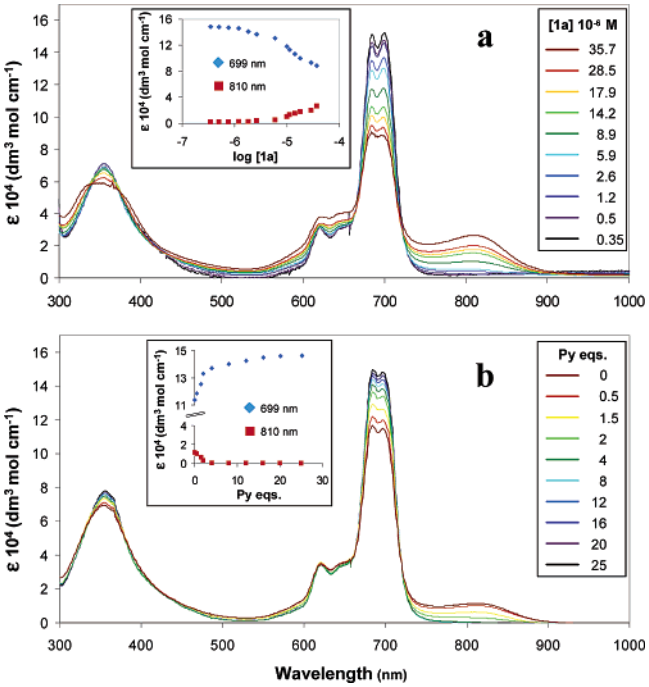


***Figure 3.*** Effect of (a) dilution and (b) addition of pyridine equivalents ([**1a**] = 1.4 $10^{-5}$ M) on the absorption spectrum of **1a** in benzonitrile and (insets) on the extinction coefficient of **1a** at 699 or 810 nm.

supported by the fact that only a few equivalents of pyridine are necessary to destroy the aggregation. In contrast, *o*-DCB or toluene solutions disclose very broad features that extend from 550 to 850 nm. We believe that, in these aromatic solvents, intermolecular stacking is much stronger than that in benzonitrile, since (i) the *Q*-band broadening persists even after diluting to the micromolar range and below (see Figures S11−S14) and (ii) the breaking of the aggregates required a higher amount of pyridine equivalents than in benzonitrile at similar concentrations.

In addition to being a powerful tool to study the aggregation of chromophores, UV−vis absorption experiments may provide valuable hints about the topology of the aggregates.[24,26] The direction and magnitude of the transition shifts due to chromophoric stacking is generally interpreted by the molecular exciton approximation developed by Kasha.[27] This model, which neglects electronic overlap of the $\pi$-systems, is based on the interaction between localized transition dipole moments. The coupling gives rise to a splitting of the monomer state into a higher energy and a lower energy contribution. The resulting spectral shift value ($\Delta\nu$) is given by

$$\Delta\nu = \frac{(N-1)}{N} \cdot \frac{M^2(1-3\cos^2\alpha)}{hr^3}$$

where $N$ is the degree of aggregation, $h$ is Planck's constant, $M$ is the transition dipole moment of the monomer, $r$ is the center-to-center distance between molecules, and $\alpha$ is the tilt angle between the polarization axis of a unit molecule and the line connecting the molecular centers. In the region $90° > \alpha > 54.7°$, $\Delta\nu$ has a positive value which brings about blue shifts of absorption wavelengths (the so-called H-type aggregates). In contrast, in the situation $54.7° > \alpha > 0°$, $\Delta\nu$ has a negative value, resulting in red spectral shifts (J-type aggregates).

In this context, it is interesting to note that both compounds **1a** and **1c** present red shifts of the dimer absorption bands in benzonitrile, with respect to the *Q*-band maximum of the monomer. This indicates that the stacked Pc $\pi$-systems, especially in the case of **1a**, are considerably tilted with respect to each other and, therefore, may overlap at least part of the AQ moiety. This tilting is not surprising since the Pc macrocycles, bearing voluminous *tert*-butyl groups in three of the isoindole units, would be forced to sacrifice a complete $\pi-\pi$ overlap in order to avoid steric repulsion.[28] In fact, model compound **2** also shows red-shifted bands upon aggregation (Figure S7).[29] Bathochromically shifted dimeric bands, though unusual, have also been observed for Pcs bearing very voluminous metals (such as Pb or Sb) or axial substituents that prevent a complete cofacial overlap of the $\pi$-systems.[24,26a,30] Triad **1b**, in contrast, presents a blue-shifted band around 630 nm, typical of most aggregated Pc systems[24] that suggests a much wider tilt angle between the macrocycles.

**B. Electrochemistry.** Solution electrochemistry of triads **1a**−**c**; model Pc compounds **2** and tetra-*tert*-butyl-phthalocyaninatozinc(II) (ZnPc($^t$Bu)$_4$); and anthraquinone derivatives **4a**−**c**, **6a**−**c**, and AQ in THF or *o*-DCB was studied by cyclic voltammetry (CV, Figures S15 and S17) and Osteryoung square wave voltammetry (OSWV, Figures 4 and S16). The potential data are summarized in Table 1.

The voltammograms of triads **1a**−**c** in THF show several features that may be attributed to each one of the electroactive moieties, even if marked differences with respect to the model Pc and AQ compounds should be noted. Careful comparison of the potential values derived from OSWV experiments (Table 1) leads to the following observations. The two Pc units in triads **1a**−**c** oxidize at the same potential, and no splitting of the first or second Pc-based oxidation processes is observed. This indicates that the two Pc moieties in the triads are electrochemically equivalent in the noncharged state. For the first oxidation process, triads **1a**−**c** are much easier to oxidize than Pc **2** by 100−140 mV, and **1c** or **1a** is easier to oxidize than **1b**. This trend (**2** > **1b** > **1a** ≈ **1c**) seems to follow the extent of $\pi$-conjugation in each compound. However, the second oxidation potential follows a different trend, i.e., **1b** > **2** ≈ **1a** ≈ **1c**. It does not differ considerably with respect to Pc **2** for triads **1a** and **1c**; however, for **1b**, a positive shift of about 52 mV was observed, indicating a much stronger inter-Pc subunit interaction in **1b** at the monopositively charged state (i.e., Pc$^{\bullet+}$−Pc$^{\bullet+}$). The cofacial arrangement of the macrocycles is likely to be responsible for these effects. At the same time, from the cathodic potentials obtained for triads **1a**−**c** and the model compounds, it should be underlined that, while no significant interactions between the AQ and Pc moieties were found for

(26) (a) Katayose, M.; Tai, S.; Kamijima, K.; Hagiwara, H.; Hayashi, N. *J. Chem. Soc., Perkin Trans. 2* **1992**, 403−409. (b) Kroon, J. M.; Koehorst, R. B. M.; van Dijk, M.; Sanders, G. M.; Sudhölter, E. J. R. *J. Mater. Chem.* **1997**, *7*, 615−624.

(27) (a) McRae, E. G.; Kasha, M. *J. Chem. Phys.* **1958**, *28*, 721. (b) Kasha, M.; Rawls, H. R.; El-Bayoumi, M. A. *Pure Appl. Chem.* **1965**, *11*, 371.

(28) To have a clearer scheme about the structure of the dimers, we carried out some 2D NMR experiments (NOESY and ROESY) on **1a**, **1b**, and **1c** in toluene-$d_8$, but the concentrations employed (ca. $10^{-3}$ M) are too high to observe defined signals of the aromatic protons and, in the best cases, only broad signals from the protons of the *tert*-butyl groups were detected.

(29) The aggregation behaviour of Pc compound **2** is different from that of the symmetrically substituted analogue ZnPc($^t$Bu)$_4$. See: Fernandez, D. A.; Awruch, J.; Dicelio, L. E. *J. Photochem. Photobiol.* **1996**, *63*, 784−792.

(30) (a) Yoon, M.; Cheon, Y.; Kim, D. *Photochem. Photobiol.* **1993**, *58*, 31. (b) Isago, H. *Chem. Commun.* **2003**, 1864−1865.

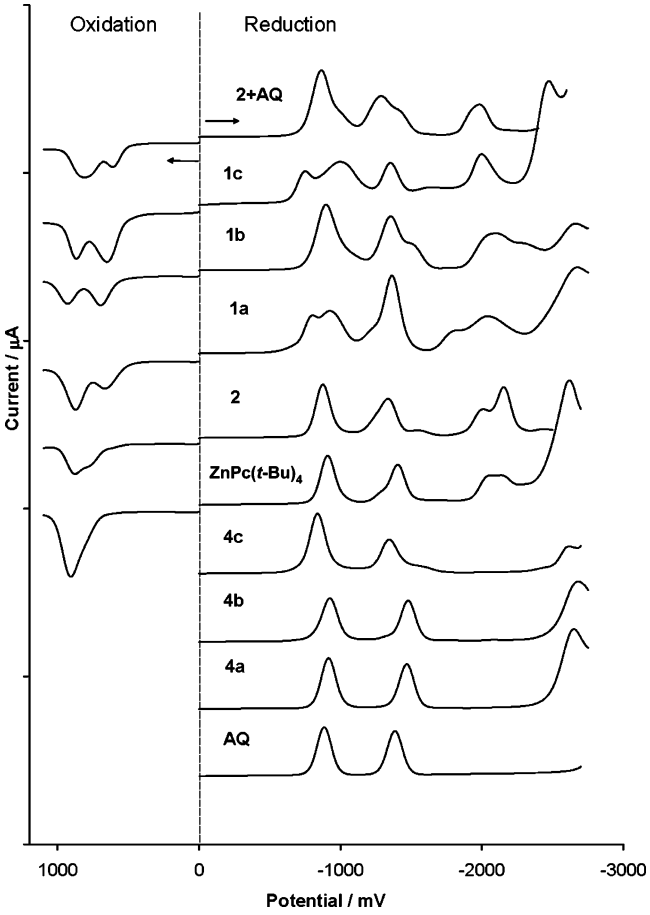


***Figure 4.*** OSWVs for **2** + AQ (1:1), **1a**−**c**, **2**, ZnPc($^t$Bu)$_4$, **4a**−**c**, and AQ in the THF−TBAPF$_6$ system at room temperature (anodic scan up to +1.1 V and cathodic scan up to −2.75 V).

**1b** (due to the cofacial arrangement of the Pcs), isomers **1a** and **1c** do display relevant shifts in the potentials of the first reductive events, negative for the Pcs and positive for the AQ unit. For example, the first reduction potential of compound **1a** is shifted by 80 mV or 112 mV with respect to those of **4a** or AQ, whereas the first reduction of the Pc moieties is shifted by 48 mV vs **2**. Similarly, triad **1c** exhibits positive shifts for the first reduction, with regards to reference compounds **4c** and AQ, on the order of 76 mV and 120 mV, respectively. The first Pc potential of **1c** was likewise negatively shifted by 200 mV or 164 mV in comparison with **2** or ZnPc($^t$Bu)$_4$, in that order. In addition, the ethenyl reduction peak in **1c** was found to shift to less negative potentials (by ca. 150 mV) than that of **4c**.

In conclusion, the electrochemical experiments in THF, where the triads do not tend to aggregate, show significant intramolecular electronic interactions in the ground state between the different subunits. The HOMO and LUMO levels, respectively, located on the Pc and AQ units, suffer a stabilization effect that parallels the red-shifts observed in the electronic absorption spectra. More concretely, the gap between the first oxidative and reductive potentials of the triads increases in the order **1b** (1.59 V) $\gg$ **1a** (1.46 V) > **1c** (1.42 V), as a result of the higher degree of in-plane $\pi$-conjugation in the extended compounds.

The main interest in these studies was the search for possible interactions between the electroactive subunits in the ground state, not only within the molecule but also at the intermolecular level within $\pi$-stacks. Therefore, we also carried out voltammetric experiments in aromatic solvents, such as *o*-DCB, where the molecules tend to form aggregates. However, at the usual concentrations of these measurements ($\sim 10^{-3}$ M), aggregation was too strong and the compounds could not be dissolved easily. As a consequence, the cathodic part of the voltammograms obtained had a poor resolution, and no clear assignments could be made. In the anodic scan, however, several oxidation peaks could be detected in *o*-DCB (see Figure S17). The first two oxidation processes of **2** were not resolved in this aromatic solvent, and only one two-electron wave was observed instead. Owing to the extended anodic window (0−1.6 V), a second wave was found around 1270−1520 mV for model Pc **2** and triads **1a**−**c**. The experiments performed in this solvent led to the following results: (i) the first oxidation potential is positively shifted with respect to Pc **2** by about 3 mV, 80 mV, and 133 mV (OSWV values) in the order **1b** << **1a** < **1c**; (ii) the second oxidation wave is found at much higher potentials than those in THF and is displaced in the same direction and the same order as above by 62 mV, 212 mV, and 244 mV (vs **2**). These results sharply contrast with the experiments in THF and shows important solvent effects, which can further affect the inter- and/or intramolecular electronic interactions of the Pc or AQ subunits in the triads.

Additional experiments were carried out with equimolar mixtures of **2** or ZnPc($^t$Bu)$_4$ with AQ in THF and *o*-DCB. While no changes were found in the potential values of ZnPc($^t$Bu)$_4$ in both anodic and cathodic scans, a similar trend to that noted for the triads **1a**−**c** was observed in the mixture of **2** and AQ in the anodic scan in THF (see Figure 4 and Table 1); i.e., **2** becomes much easier to oxidize after mixing with AQ, showing a negative shift of about 180 mV for the first and 70 mV for the second oxidation process. This suggests some kind of ground-state intermolecular interaction between Pc **2** and AQ at the concentration of the electrochemical experiments ($\sim 10^{-3}$ M).[31] In contrast, in *o*-DCB, where the aggregation between Pc molecules is notable, no significant changes were found in the mixtures of **2** or ZnPc($^t$Bu)$_4$ with AQ.

**Excited States. A. Steady-State Fluorescence Spectroscopy.** The fluorescence features of the employed ZnPc reference **2** include a quantum yield of 0.3 and a lifetime of 3.4 ns. Figure S18 exemplifies that relative to this strongly fluorescing reference, the ZnPc fluorescence in **1a**−**c** is strongly quenched. As excitation wavelength we used for all samples 680 nm, which ensures the selective *Q*-band excitation of the ZnPc moieties. Any 9,10-anthraquinone excitation is impossible.

For **1b**, which is soluble in toluene, THF, *o*-DCB, and benzonitrile at the concentration of the photophysical experiments, a quenching behavior is seen that depends strongly on the solvent polarity. The fluorescence quenching in benzonitrile is nearly 6.5 times stronger than that in toluene, for which we determined a quantum yield of $1.0 \times 10^{-1}$. THF ($\Phi = 4.5 \times 10^{-2}$) and *o*-DCB ($\Phi = 1.7 \times 10^{-2}$) fall between the cases of toluene and benzonitrile.

Based on the solvent dependence we postulate that the accelerated singlet excited-state deactivation in **1b** originates from an intramolecular electron transfer. Further support for this notion is borrowed from the electrochemical determination of

(31) However, no hints of intermolecular interactions between **2** and AQ were found in UV−vis titration experiments.

***Table 1.*** Electrochemical Data (mV vs Fc) of the Redox Processes of Compounds **1a**−**c**, **2**, ZnPc($^t$Bu)$_4$, **4a**−**c**, AQ, and **2** + AQ Detected by OSWV in THF or *o*-DCB Solutions at Room Temperature under Identical Experimental Conditions[a]

| | Solvent | $E_{ox}^{1\,P}$ | $E_{ox}^{2\,P}$ | $E_{red}^{1}$ | $E_{red}^{2}$ | $E_{red}^{3}$ | $E_{red}^{4}$ | $E_{red}^{5}$ | $E_{red}^{6}$ |
|---|---|---|---|---|---|---|---|---|---|
| **1a** | THF | 662 (2e) | 872 (2e) | -804$^{A}$ | -924 (2e)$^{P}$ | | -1364 (3e)$^{P,A}$ | -2042$^{(a)}$(4e)$^{P}$ | -2676$^{V}$ |
| **1b** | | 696 (2e) | 928 (2e) | -898 (3e)$^{P,A}$ | | | -1356$^{(a)}$(3e)$^{P,A}$ | -2098$^{(a)}$(4e)$^{P}$ | -2664$^{V}$ |
| **1c** | | 652 (2e) | 868 (2e) | -764$^{A}$ | -1076 (3e)$^{P,A}$ | | -1376 (2e)$^{P}$ | -2024 (4e)$^{P}$ | -2472$^{V}$ |
| **2** | | 790 | 876 | -876 | -1336 | -2008 | -2154 | | |
| ZnPc($^t$Bu)$_4$ | | 912 (2e) | | -912 | -1404 | -2064 | -2620 | | |
| **4a** | | | | -916 | -1470 | | | | -2652$^{V}$ |
| **4b** | | | | -926 | -1480 | | | | -2682$^{V}$ |
| **4c** | | | | -840 | -1348 | | | | -2620$^{V}$ |
| AQ | | | | -884 | -1376 | | | | |
| **2**+AQ | | 612 | 808 | -864 (2e)$^{P,A}$ | | -1288$^{P}$ | -1428$^{A}$ | -1984$^{P}$ | |
| **1a** | *o*-DCB | 688 (2e) | 1484 | Poorly resolved reduction waves | | | | | |
| **1b** | | 611 (2e) | 1334 | | | | | | |
| **1c** | | 741 (2e) | 1516 | | | | | | |
| **2** | | 608 (2e) | 1272 | | | | | | |

[a] P: Pc-based redox process. A: AQ-based redox process. V: Reduction of the vinyl group. (a): These waves are accompanied by a small, nonresolvable shoulder.

the reduction and oxidation potential of the AQ and ZnPc moieties in **1b**, respectively. Neglecting Coulombic interactions, we estimate the energy of the charge-separated state in THF as 1.59 eV, by simply adding the redox potential. Relative to the ZnPc singlet excited state in **1b** (i.e., average between longest wavelength absorption at 1.81 eV and shortest wavelength emission at 1.78 eV is 1.80 eV), this corresponds to a moderate electron-transfer energy gap (i.e., $-\Delta G$) of 0.20 eV. Also the excited-state energies should be compared to evaluate alternative energy transfer reactions. The singlet excited-state energies of ZnPc and AQ are 1.80 and 2.94 eV, respectively. The corresponding triplet energies are 1.13 eV for ZnPc and 2.7 eV for AQ. With these energies in hand we can rule out an intramolecular transduction of singlet excited state energy, which would be highly endothermic (i.e., $-\Delta G = -1.13$ eV). Similarly a thermodynamically driven singlet−triplet energy transfer is unlikely to take place (i.e., $-\Delta G = -0.89$ eV).

Next, we would like to discuss **1a**. Overall the ZnPc-centered fluorescence, for example, in THF is more strongly quenched than that for **1b**. The difference is a factor of 4. Going back to the electrochemistry, the energy of the charge-separated state is estimated as being 1.46 eV, slightly lower than that seen for **1b**. Consequently, the stronger fluorescence quenching evolves from a larger energy gap, as well as from a higher degree of $\pi$-conjugation between the donor and acceptor components. The fluorescence experiments were limited to THF and benzonitrile, since the solubility of **1a** in *o*-DCB or toluene was not satisfactory. In line with an electron-transfer deactivation, the ZnPc fluorescence in benzonitrile is further quenched.

Finally, we come to **1c**, which shows the strongest fluorescence quenching among the tested donor−acceptor ensembles. In THF and benzonitrile the quantum yields are $8.4 \times 10^{-3}$ and $7.9 \times 10^{-4}$. Importantly, the singlet excited state energy is only 1.77 eV, due to the bathochromic shifts of absorption and emission. Besides a large energy gap ($-\Delta G = 0.35$ eV), the chemical linkage should be considered. Attachment of the double bond to the beta positions leads to an enhanced electronic coupling of ZnPc to the central quinone ring relative to **1a**, as demonstrated in ground-state absorption and voltammetric experiments. Both parameters are believed to be central in facilitating the electron-transfer process from the photoexcited ZnPc to the electron accepting quinoid part.

**B. Time-Resolved Fluorescence Spectroscopy.** In time-resolved fluorescence decay measurements, lifetimes of 3.4 ± 0.5 ns are registered for reference **2** in THF. This is different for **1a** and **1c** in THF. For example, when applying a satisfying monoexponential fit (i.e., $\chi^2 \approx 1$) for the emission-time profiles for **1a**, a lifetime of 0.12 ± 0.1 ns was determined. The absolute difference in lifetimes between reference **2** and **1a** agrees well with the steady-state quenching factor of 30 (i.e., **2**: $\Phi = 0.3$; **1a**: $\Phi = 1.1 \times 10^{-2}$). For **1c** we must assume an even shorter lifetime, which is covered by the instrumental time resolution of around 0.1 ns. This trend also fits with the steady-state results; that is, **1c** has the lowest fluorescence quantum yield of $8.4 \times 10^{-3}$.

A surprising result stems from experiments with **1b** in THF, where the molecular topology forces the $\pi-\pi$ stacking and the absorption spectra reveal excitonic broadening. In particular, we determine a lifetime of 3.1 ± 0.2 ns. This clearly contradicts the THF measurements with **1a** and **1c**, where lifetimes of ∼0.1 ns were registered. We must, however, assume the existence of a major short-lived component that would lie outside of the detection range (vide infra).[32] A possible rationale for this observation is ZnPc aggregation (in the form of $\pi-\pi$ stacking, accompanied by exciton coupling) as witnessed in the ground-state absorption spectra. Long-lived fluorescence decay com-

ponents, attributed to stacked species, have also been observed in some phthalocyanines[30a] and in conjugated polymers.[33]

**C. Transient Absorption Spectroscopy.** The fluorescence studies infer that a solvent-dependent and rapid electron transfer prevails in **1a**−**c**. To shed light onto the mechanism by which the ZnPc singlet excited states in **1a**−**c** deactivate and to find spectroscopic conformation for the $ZnPc^{\bullet+}/AQ^{\bullet-}$ radical ion pair state formation, complementary transient absorption measurements were necessary (i.e., with femtosecond through millisecond time resolution).

In particular, when photoexciting **2** in either THF or benzonitrile with 150 fs laser pulses, differential absorption changes develop (i.e., $(1.4 \pm 0.2) \times 10^{12}$ $s^{-1}$) in the range between 400 and 800 nm that reveal the following singlet excited-state characteristics: weak transient absorption in the 430−580 nm region and strong transient minima at 610 and 680 nm. Important is that both minima correspond to the maxima seen in the ground-state absorption spectrum. The transient characteristics are completed by a near-infrared transition that centers around 820 nm (Figure S19).[34] The ZnPc singlet excited state is metastable, and kinetic analysis throughout the 400−800 nm range yielded a singlet lifetime of 3.1 ± 0.2 ns reflecting an intersystem crossing (between the singlet excited and triplet excited manifolds) rate of $(3.2 \pm 0.5) \times 10^8$ $s^{-1}$. A characteristic spectrum of the latter is shown in Figure S20 and includes maxima at 550 nm and minima at 690 nm. Notably, in the near-infrared region (i.e., 750−1100 nm) no distinct features are seen.

A series of transient absorption spectra for **1a**−**c** in either THF or benzonitrile are collected in Figures 5−7 and S21−S23. Before, however, discussing dynamic or mechanistic aspects the shape of the transient bleach in the 600−800 nm section should be elucidated. Compound **1c**, for example, reveals in THF, reminiscent to what is seen for **2**, a set of sharp minima at 678 and 700 nm. In benzonitrile, on the other hand, a significant broadening is discernible with a tail that reaches far beyond our instrumental detection limit of 800 nm. For **1a** the same differences arise between THF and benzonitrile as solvents. Finally, when inspecting **1b** similarly broad bleaching is seen in both solvents. Overall, the aforementioned observations corroborate our absorption and fluorescence experiments, that is, strongly inferring the susceptibility of the phthalocyanine core to form $\pi-\pi$ stacks, which are either topographically (i.e., **1b**) or solvent enforced (i.e., benzonitrile).

In the case of **1a**−**c**, the transients at very early times are practically identical to those that have been described for **2**. In particular, we see the singlet excited state formed with an ultrafast dynamics of $(1.6 \pm 0.2) \times 10^{12}$ $s^{-1}$. However, instead of seeing the slow intersystem crossing dynamics, the lifetimes of the singlet excited states are governed by rapid intramolecular decays. The decay time profiles are, in large part, monoexponential (see for representative profiles Figures 6 and 7), and from fitting them we determined rates that vary between $1.0 \times 10^{10}$ and $4.4 \times 10^{10}$ $s^{-1}$. Notably, as Table 2 demonstrates these values are in excellent agreement with the extrapolation of the fluorescence data. The transient absorption changes, recorded at the conclusion of the fast deactivation, show characteristics that are distinctly different from the ZnPc triplet features. In particular, we see features of the one-electron reduced anthraquinone (i.e., $AQ^{\bullet-}$) and of the one-electron oxidized ZnPc moieties (i.e., $ZnPc^{\bullet+}$). $AQ^{\bullet-}$ are characterized by transient maxima that depend on the anthraquinone substitution pattern but are typically located in the 500 nm region[35] (i.e., **1a**, 510 nm; **1b**, 510 nm; **1c**, 505 nm). On the other hand, $ZnPc^{\bullet+}$ reveals in the recorded region maxima at around 590 nm and minima around 690 nm. Additionally, a near-infrared fingerprint at 840 nm, which also reflects the one-electron oxidized ZnPc, has been seen in complementary nanosecond experiments (vide infra).

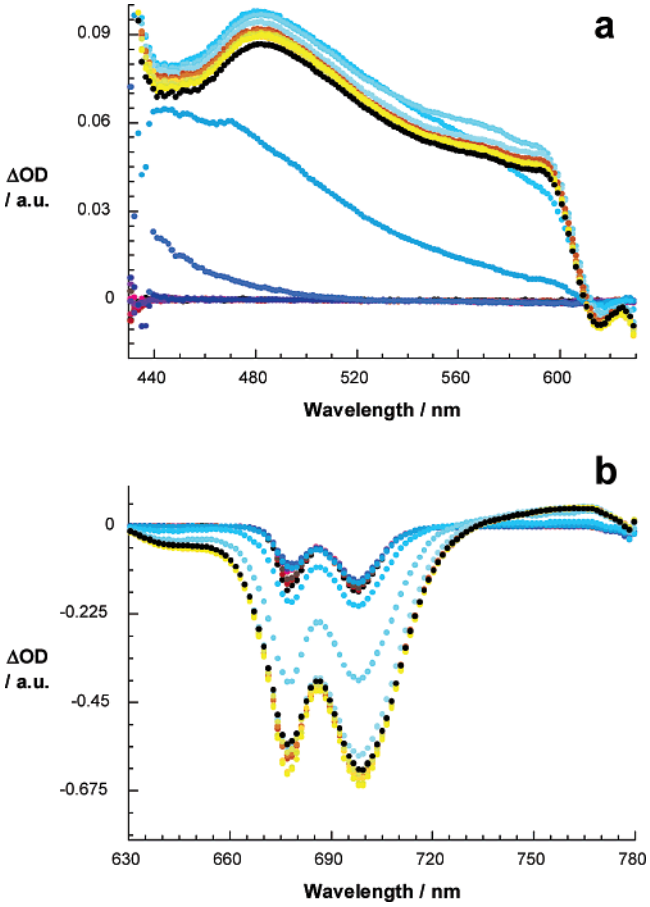


***Figure 5.*** Differential absorption spectrum (visible) obtained upon femtosecond flash photolysis (387 nm) of ~$1.0 \times 10^{-5}$ M solutions of **1c** in THF with several time delays between 0 and 200 ps at room temperature, monitoring the formation of the $ZnPc^{\bullet+}/AQ^{\bullet-}$ radical ion pair state.

A closer inspection of the short time scales reveals that for **1a** and **1c** in benzonitrile the $10^{10}$ $s^{-1}$ kinetics consist of two components. The two such processes are, however, not seen for **1b** in THF or benzonitrile or for **1a** and **1c** in THF. This could be rationalized with weak phthalocyanine interactions in the tilted dimer configuration of **1a** and **1c**, which is postulated based on the ground-state absorption (vide supra) and subsequent delocalization of the radical cation over two ZnPc moieties.

(32) When testing **1a**−**c** in benzonitrile surprising results were gathered. Despite the lower quantum yields the emission−time profiles were best fitted (i.e., $\chi^2 \approx 1$) by a monoexponential decay function that yields lifetimes of 3.5 ± 0.5 ns (**1a**), 3.1 ± 0.2 ns (**1b**), and 2.9 ± 0.5 ns (**1c**). The authors would like to point out that, in the experiments in benzonitrile, much lower signal intensities (with respect to those in THF) were noted. No traces of Pc **2** contamination were found in the samples of **1a**−**c**.

(33) Belletête, M.; Bouchard, J.; Leclerc, M.; Durocher, G. *Macromolecules* **2005**, *38*, 880−887.

(34) This maximum was determined in our previous work with picosecond resolved transient absorption measurements.

(35) McCafferty, D. G.; Friesen, D. A.; Danielson, E.; Wall, C. G.; Saderholm, M. J.; Erickson, B. W.; Meyer, T. J. *Proc. Natl. Acad. Sci. U.S.A.* **1996**, *93*, 8200−8204.

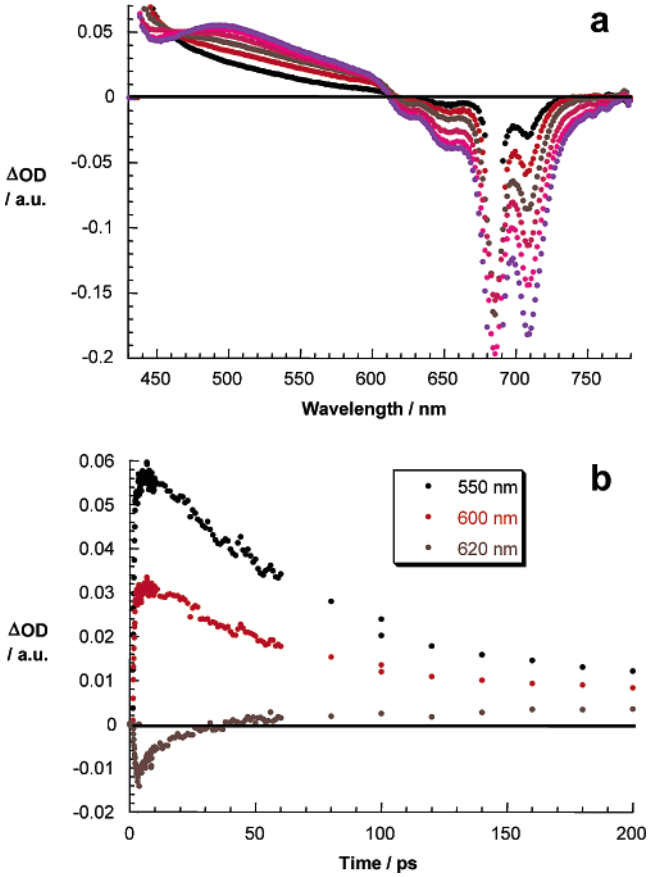


***Figure 6.*** (a) Differential absorption spectra (visible) obtained upon femtosecond flash photolysis (387 nm) of **1c** in benzonitrile with several time delays between 0 and 10 ps at room temperature. (b) Time−absorption profiles of the spectra shown above at 550, 600, and 620 nm, monitoring the formation of the $ZnPc^{\bullet+}/AQ^{\bullet-}$ radical ion pair state.

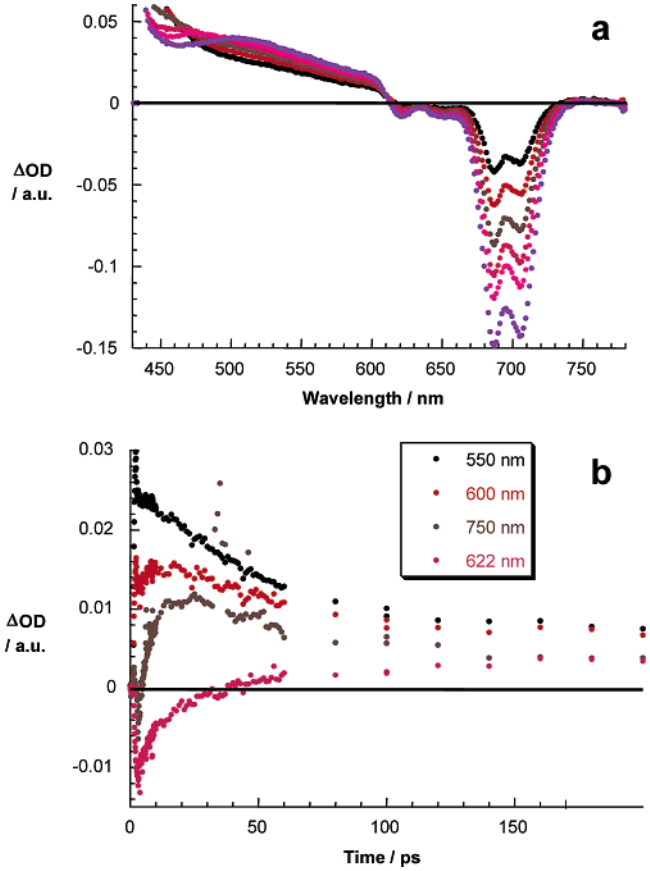


***Figure 7.*** (a) Differential absorption spectra (visible) obtained upon femtosecond flash photolysis (387 nm) of **1a** in benzonitrile with several time delays between 0 and 10 ps at room temperature. (b) Time−absorption profiles of the spectra shown above at 550, 600, 622, and 750 nm, monitoring the formation of the $ZnPc^{\bullet+}/AQ^{\bullet-}$ radical ion pair state.

Apparently, these interactions are much stronger when the two phthalocyanines orient face-to-face as in **1b**, and consequently, no distinctions are possible in the kinetic traces.

All radical pair attributes (i.e., $AQ^{\bullet-}$, around 500 nm; $ZnPc^{\bullet+}$, maxima at around 590 nm and minima around 690 nm) are stable on the femtosecond time scale; see Figures S24 and S25. To examine the charge-recombination dynamics the same solutions of **1a**−**c** were excited with a 6 ns laser pulse. In this context, the spectral fingerprints of $AQ^{\bullet-}$ in the 500 nm region[35] and that of $ZnPc^{\bullet+}$ around 840 nm (Figures 8 and S26), as seen immediately after the ns laser pulse, are useful probes.

In THF, for example, we derived for **1a** a relative short radical pair lifetime of 26 ± 2 ns (Figure S27). This changed drastically when looking at benzonitrile solutions, where significant stabilizations of the radical ion pair features were deduced for **1a**. A lifetime of 20.3 $\mu$s, which is 3 orders of magnitude larger than that in THF, testifies to the valuable effects stemming from the $\pi-\pi$ stacking. It should be mentioned that due to the aggregated status of **1a** in benzonitrile the transient features are somewhat broader, which is usually interpreted in terms of intermolecular delocalization of the radical ions within the stacks.[6a,b] Hence, the $\pi-\pi$ stacks facilitate the rapid intermolecular $ZnPc^{\bullet+}$ and $AQ^{\bullet-}$ delocalization (i.e., between molecules in the same $\pi-\pi$ stack) and, in turn, prevents the fast charge recombination seen in THF.

On the other hand, the radical ion pair lifetimes for **1c** in THF must be on the lower nanosecond/picosecond time scale (i.e., < 10 ns), due to the lack of $ZnPc^{\bullet+}/AQ^{\bullet-}$ features. It is feasible to assume that the good electronic coupling between the redox-active moieties, which has been shown to expedite the charge separation process, is also responsible for the acceleration of the charge recombination kinetics. In benzonitrile, again, a long-lived (43 ± 2 $\mu$s) decay was registered. Some typical time-absorption profiles for **1c** in benzonitrile are gathered in Figure S28a.

Interestingly, in the molecularly enforced $\pi-\pi$ stacks (i.e., **1b**), analysis of the radical pair lifetime yielded a value of 87 ± 5 ns in THF. Relative to **1a** or **1c**, which can be regarded as the unfolded conformer of **1b**, this corresponds to more than a 3-fold stabilization of the charge-separated state. It is important to note that under these experimental conditions the $ZnPc^{\bullet+}$ stabilization in **1b** can only occur between the two ZnPc moieties that reside in close contact (i.e., intramolecular). However, the greatest difference comes from the experiments in benzonitrile, where the radical pair of compound **1b** shows only a slight stabilization (105 ± 5 ns; see Figure S28b) when compared with the extended systems in **1a** and **1c**, where the coupling is mostly based on long-range intermolecular interactions. Table 2 summarizes the most relevant data obtained in the photophysical experiments.[36]

(36) To confirm the intramolecular charge recombination dynamics we probed **1a**−**c** at different laser powers and different concentrations. Regardless of the experimental conditions, the best fits were obtained by applying unimolecular decay functions that gave rise to the same charge recombination rate constants.

***Table 2.*** Photophysical Properties of **1a**−**c** in Room Temperature THF and Benzonitrile (bzcn) Solutions

| feature | solvent | **2** | **1a** | **1b**[a] | **1c** |
|---|---|---|---|---|---|
| fluorescence quantum yield ($\Phi_F$) | THF | 0.3 | $1.1 \times 10^{-2}$ | $4.5 \times 10^{-2}$ | $8.4 \times 10^{-3}$ |
| | bzcn | 0.3 | $3.8 \times 10^{-3}$ | $1.5 \times 10^{-2}$ | $7.9 \times 10^{-4}$ |
| fluorescence lifetime ($\tau_F$) | THF | $3.4 \pm 0.5$ ns | $0.12 \pm 0.1$ ns | $3.1 \pm 0.2$ ns | <0.1 ns |
| | bzcn | $3.4 \pm 0.5$ ns | $3.5 \pm 0.5$ ns | $3.1 \pm 0.2$ ns | $2.9 \pm 0.5$ ns |
| singlet decay (fluorescence), $s^{-1}$ | THF | | $8.8 \times 10^9$ | $2.1 \times 10^{10}$ | $1.1 \times 10^{10}$ |
| | bzcn | | $2.6 \times 10^{10}$ | $6.6 \times 10^{10}$ | $1.2 \times 10^{11}$ |
| singlet decay (transient), $s^{-1}$ | THF | | $1.0 \times 10^{10}$ | $2.5 \times 10^{10}$ | $1.7 \times 10^{10}$ |
| | bzcn | | $3.2 \times 10^{10}$ | $3.3 \times 10^{10}$ | $4.4 \times 10^{10}$ |
| radical pair lifetime ($\tau_{CR}$) | THF | | $26 \pm 2$ ns | $87 \pm 5$ ns | <10 ns |
| | bzcn | | $20 \pm 2$ $\mu$s | $105 \pm 5$ ns | $43 \pm 2$ $\mu$s |

[a] Fluorescence quantum yields are $1.0 \times 10^{-1}$ in toluene and $1.7 \times 10^{-2}$ in *o*-DCB.

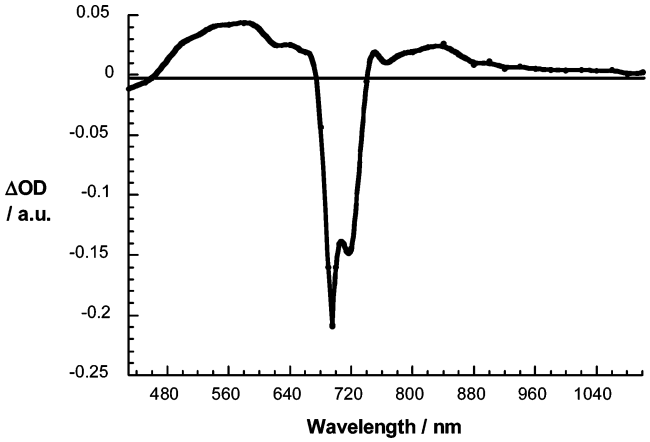


***Figure 8.*** Differential absorption spectra (near-infrared) obtained upon nanosecond flash photolysis (355 nm) of $\sim 1.0 \times 10^{-5}$ M solutions of **1a** in nitrogen-saturated benzonitrile with a time delay of 100 ns, showing the radical anion and radical cation features of $AQ^{\bullet -}/ZnPc^{\bullet +}$, respectively.

## Summary and Conclusions

We have prepared three isomeric donor-acceptor systems in which two phthalocyanine units are connected to a central anthraquinone moiety through the 1-,5- (**1a**), 1-,8- (**1b**) or 2-,6- (**1c**) positions, leading to markedly different packed (**1b**) or extended (**1a** and **1c**) topologies. As a result, these triads show distinct ground- and excited-state electronic interactions between the Pc donors and the AQ acceptor, at both the intramolecular and the intermolecular level. In triad **1b**, the ZnPc units are forced to $\pi$-stack cofacially and out of the plane of the AQ ring. Consequently, this molecule shows strong inter-Pc interactions, that give rise to intramolecular excitonic coupling but a relatively small electronic communication with the AQ acceptor through the vinyl spacers. On the opposite side, the 1-,5- or 2-,6-connections of triads **1a** and **1c** allow for an efficient $\pi$-conjugation between the Pc and AQ active units that extends over the entire planar system. These two molecules show a strong tendency to aggregate in solution by $\pi-\pi$ stacking, giving rise to J-type oligomers. The degree of aggregation of these two triads could be limited to small oligomers (mostly dimers) by the introduction of bulky *tert*-butyl groups in the peripheral Pcs and by the proper choice of the solvent media. Photoexcitation of the Pc units of **1a**−**c** results in the formation of the $Pc^{\bullet +}-AQ^{\bullet -}$ charge transfer state. We have demonstrated that the kinetics of these electron transfer reactions may be modified as a function of the aggregation status of the triads. For instance, for **1a** or **1c** in THF, where only monomeric species are present, the radical pair formed decays in a few nanoseconds. In benzonitrile, in contrast, small aggregates are formed and the charge-transfer state shows a huge stabilization, its lifetime increasing more than 3 orders of magnitude. The special equilibrium between monomers and small oligomers taking place in this solvent is likely to be the cause for these effects, since the radical ions formed can be stabilized within the J-type stacks and may even migrate or diffuse. A next logical step in this line of research would be to increase the size of the aggregates to the nanometer scale and beyond, so that charges may migrate over longer distances, by profiting from the exceptional properties of phthalocyanines and other planar $\pi$-systems as columnar mesogens.

## Experimental Section

**1,5-Bis[ethen(tri-*tert*-butylphthalocyaninatozinc(II))-yl]-9,10-anthraquinone (1a), 1,8-Bis-[(ethen(tri-*tert*-butylphthalocyaninatozinc-(II))-yl]-9,10-anthraquinone (1b), and 2,6-Bis-[(ethen(tri-*tert*-butylphthalocyaninatozinc(II))-yl]-9,10-anthraquinone (1c): General Procedure:** A mixture of tri-*tert*-butyl-vinylphthalocyaninatozinc(II) (**2**) (46 mg, 0.06 mmol), the corresponding diiodoanthraquinone **3a**−**c** (11.5 mg, 0.025 mmol), $(MeCN)_2PdCl_2$ (0.5 mg, 0.0019 mmol), tetrabutylammonium bromide (9.8 mg, 0.03 mmol), and triethylamine (0.1 mL) in dry toluene (10 mL) was heated at 100 °C under argon for 48 h. The solvent was removed under reduced pressure, and the crude product was purified by flash chromatography ($SiO_2$, hexane/THF 2:1 for **1a** and **1c**, 3:1 for **1b**). The solid obtained was then washed with methanol and hexane, in that order, and dried under a vacuum.

**1a:** Yield: (33 mg, 75%), green solid. Mp > 250 °C. $^1$H NMR (300 MHz, [$d_8$]THF, 25 °C, TMS): $\delta = 9.5-7.5$ (m, 34H; arom. and vinyl), 2.1−1.8 (m, 54H; $C(CH_3)_3$). FT-IR (KBr): $\nu = 2953, 1663, 1613, 1578, 1487, 1391, 1328, 1255, 1147, 1088, 1047, 921, 828, 746$ cm$^{-1}$. UV/vis (THF): $\lambda_{max}$ (log $\epsilon$) = 690 (5.15), 674 (5.08), 350 (4.93) nm. MS (MALDI-TOF, dithranol): $m/z = 1744-1753$ $[M]^+$. Anal. Calcd (%) for $C_{106}H_{88}N_{16}O_2Zn_2$: C, 72.81; H, 5.07; N, 12.82. Found: C, 72.32; H, 4.79; N, 12.45.

**1b:** Yield: (31 mg, 72%), green solid. Mp > 250 °C. $^1$H NMR (300 MHz, [$d_8$]THF, 25 °C, TMS): $\delta = 9.5-7.5$ (m, 34H; arom. and vinyl), 2.1−1.8 (m, 54H; $C(CH_3)_3$). FT-IR (KBr): $\nu = 2954, 1671, 1613, 1584, 1488, 1392, 1328, 1256, 1149, 1089, 1047, 921, 831, 747$ cm$^{-1}$. UV/vis (THF): $\lambda_{max}$ (log $\epsilon$) = 683 (5.0), 348 (4.90) nm. MS (MALDI-TOF, dithranol): $m/z = 1744-1753$ $[M]^+$. Anal. Calcd (%) for $C_{106}H_{88}N_{16}O_2Zn_2$: C, 72.81; H, 5.07; N, 12.82. Found: C, 73.29; H, 4.88; N, 12.49.

**1c:**[15d] Yield: (30 mg, 70%), green solid. Mp > 250 °C. $^1$H NMR (300 MHz, [$d_8$]THF, 25 °C, TMS): $\delta = 9.6-7.6$ (m, 34H, arom. and vinyl), 2.1−1.8 (m, 54H; $C(CH_3)_3$). FT-IR (KBr): $\nu = 2953, 1672, 1613, 1585, 1486, 1392, 1304, 1255, 1146, 1088, 1047, 920, 831, 747$ cm$^{-1}$. UV/vis (THF): $\lambda_{max}$ (log $\epsilon$) = 696 (5.18), 675 (5.10), 352 (4.94)

nm. MS (MALDI-TOF, dithranol): $m/z$ = 1744−1753 $[M]^+$. Anal. Calcd (%) for $C_{106}H_{88}N_{16}O_2Zn_2$: C, 72.81; H, 5.07; N, 12.82. Found: C, 72.27; H, 4.98; N, 12.33.

**1,5-Diethenyl-9,10-anthraquinone (4a), 1,8-Diethenyl-9,10-anthraquinone (4b), and 2,6-Diethenyl-9,10-anthraquinone (4c): General Procedure:** To a stirred solution of the corresponding diiodoanthraquinone **3a**−**c** (0.46 g, 1 mmol) and $Pd(PPh_3)_4$ (115.5 mg, 0.1 mmol) in toluene (20 mL) under an argon atmosphere tributyl(vinyl)tin (0.95 g, 3 mmol) was added, and the solution was heated at 100 °C for 16 h. After evaporation of the solvent the residue was extracted with $CH_2Cl_2$, washed with water, dried over $Na_2SO_4$, and evaporated under reduced pressure. The resulting solid was finally chromatographed ($SiO_2$, $CH_2Cl_2$).

**4a:** Yield: (0.21 g, 80%), yellow solid. Mp = 180−182 °C. $^1$H NMR (300 MHz, $CDCl_3$, 25 °C, TMS): $\delta$ = 8.25 [dd, $^3J$(H,H) = 7.6 Hz, $^4J$(H,H) = 1.6 Hz, 2H; H-4, H-8], 7.8 [dd, $^3J$(H,H) = 7.6 Hz, $^4J$(H,H) = 1.6 Hz, 2H; H-2, H-6], 7.75 [dd, $^3J$(H,H) = 17.2 Hz, $^3J$(H,H) = 10.8 Hz, 2H; H-15, H-17], 7.72 [t, $^3J$(H,H) = 7.6 Hz, 2H; H-3, H-7], 5.68 [dd, $^3J$(H,H) = 17.2 Hz, $^2J$(H,H) = 1.2 Hz, 2H; H-16, H-18], 5.5 [dd, $^3J$(H,H) = 10.8 Hz, $^2J$(H,H) = 1.2 Hz, 2H; H-16, H-18]. $^{13}$C NMR (75 MHz, $CDCl_3$, 25 °C, TMS): $\delta$ = 185.13, 140.75, 137.10, 135.79, 133.7, 133.56, 127.37, 117.55. FT-IR (KBr): $\nu$ = 1663, 1580, 1434, 1325, 1271, 1045, 979, 911, 823, 712 cm$^{-1}$. MS (FAB, 3-NOBA): $m/z$ = 261 $[M + H]^+$. Anal. Calcd (%) for $C_{18}H_{12}O_2$: C, 83.06; H, 4.65. Found: C, 82.88; H, 4.45.

**4b:** Yield: (0.20 g, 77%), yellow solid. Mp = 123−125 °C. $^1$H NMR (300 MHz, $CDCl_3$, 25 °C, TMS): $\delta$ = 8.24 [dd, $^3J$(H,H) = 7.6 Hz, $^4J$(H,H) = 1.5 Hz, 2H; H-4, H-5], 7.84 [dd, $^3J$(H,H) = 7.6 Hz, $^4J$(H,H) = 1.5 Hz, 2H; H-2, H-7], 7.70 [t, $^3J$(H,H) = 7.6 Hz, 2H; H-3, H-6], 7.66 [dd, $^3J$(H,H) = 17.6 Hz, $^3J$(H,H) = 10.8 Hz, 2H; H-15, H-17], 5.68 [dd, $^3J$(H,H) = 17.6 Hz, $^2J$(H,H) = 1.2 Hz, 2H; H-16, H-18], 5.48 [dd, $^3J$(H,H) = 10.8 Hz, $^2J$(H,H) = 1.2 Hz, 2H; H-16, H-18]. $^{13}$C NMR (75 MHz, $CDCl_3$, 25 °C, TMS): $\delta$ = 187.13, 184.01, 140.56, 136.96, 134.20, 133.75, 133.0, 131.79, 126.84, 117.22. FT-IR (KBr): $\nu$ = 1671, 1569, 1433, 1327, 1265, 985, 895, 850, 800, 749 cm$^{-1}$. MS (FAB, 3-NOBA): $m/z$ = 261 $[M + H]^+$. Anal. Calcd (%) for $C_{18}H_{12}O_2$: C, 83.06; H, 4.65. Found: C, 82.81; H, 4.46.

**4c:** Yield: (0.23 g, 89%), yellow solid. Mp > 250 °C. $^1$H NMR (300 MHz, $CDCl_3$, 25 °C, TMS): $\delta$ = 8.27 [d, $^4J$(H,H) = 1.8 Hz, 2H; H-1, H-5], 8.25 [d, $^3J$(H,H) = 8.1 Hz, 2H; H-4, H-8], 7.78 [dd, $^3J$(H,H) = 8.1 Hz, $^4J$(H,H) = 1.8 Hz, 2H; H-3, H-7], 6.84 [dd, $^3J$(H,H) = 17.6 Hz, $^3J$(H,H) = 10.8 Hz, 2H; H-15, H-17], 6.02 [d, $^3J$(H,H) = 17.6 Hz, 2H; H-16, H-18], 5.52 [d, $^3J$(H,H) = 10.8 Hz, 2H; H-16, H-18]. $^{13}$C NMR (75 MHz, $CDCl_3$, 25 °C, TMS): $\delta$ = 182.67, 143.21, 135.32, 133.78, 132.5, 131.24, 127.76, 124.72, 118.33. FT-IR (KBr): $\nu$ = 1674, 1592, 1413, 1297, 993, 917, 858, 758, 715 cm$^{-1}$. MS (FAB, 3-NOBA): $m/z$ = 261 $[M + H]^+$. Anal. Calcd (%) for $C_{18}H_{12}O_2$: C, 83.06; H, 4.65. Found: C, 82.84; H, 4.49.

**1,5-Bis(trimethylsilylethynyl)-9,10-anthraquinone (5a), 1,8-Bis(trimethylsilylethynyl)-9,10-anthraquinone (5b), and 2,6-Bis(trimethylsilylethynyl)-9,10-anthraquinone (5c): General Procedure:** To a stirred solution of diiodoanthraquinone **3a**−**c** (0.46 g, 1 mmol), CuI (3.8 mg, 20 $\mu$mol), and $(PPh_3)_2PdCl_2$ (14 mg, 20 $\mu$mol) in triethylamine (4 mL) and toluene (10 mL) under an argon atmosphere trimethylsilylacetylene (0.21 g, 2.2 mmol) was added, and the mixture was refluxed for 3 h. The cold solution was filtered through a bed of celite, and the solid was washed with an additional amount of toluene (5 mL). The filtrate was then washed with brine and water, and the solvent was evaporated under reduced pressure. The residual solid was washed with hot methanol, filtered, and dried.

**5a:** Yield: (0.26 g, 65%), yellow solid. Mp = 123−125 °C. $^1$H NMR (200 MHz, $CDCl_3$, 25 °C, TMS) $\delta$ = 8.33 (dd, $^3J$ = 7.6 Hz, $^4J$ = 1.6 Hz, 2H; H-4, H-8), 7.90 (dd, $^3J$ = 7.6 Hz, $^4J$ = 1.6 Hz, 2H; H-2, H-6), 7. 69 (t, $^3J$ = 7.6 Hz, 2H; H-3, H-7), 0.35 (s, 18H; $CH_3$). FT-IR (KBr): $\nu$ = 2961, 2150, 1678, 1570, 1435, 1313, 1273, 1036, 845, 764 cm$^{-1}$. MS (FAB, 3-NOBA): $m/z$ = 373 $[M + H]^+$. Anal. Calcd (%) for $C_{24}H_{24}O_2Si$: C, 77.28; H, 6.49. Found: C, 77.53; H, 6.28.

**5b:** Yield: (0.32 g, 80%), yellow-orange solid with identical physical characteristics to the ones already described.[21]

**5c:** Yield: (0.28 g, 70%), yellow solid. Mp = 180−182 °C. $^1$H NMR (200 MHz, $CDCl_3$, 25 °C, TMS) $\delta$ = 8.36 (d, $^4J$ = 1.5 Hz, 2H; H-1, H-5), 8.25 (d, $^3J$ = 8.2 Hz, 2H; H-4, H-8), 7.83 (dd, $^3J$ = 8.2 Hz, $^4J$ = 1.5 Hz, 2H; H-3, H-7), 0.29 (s, 18H; $CH_3$). $^{13}$C RMN (50 MHz, $CDCl_3$) $\delta$ = 181.9 (C=O), 136.9 (C-3, C-7), 133.4 (C-2, C-6), 132.4 (C-11, C-13), 130.7 (C-4, C-8), 129.6 (C-12, C-14), 127.3 (C-1, C-5), 103.1 (C-15, C-17), 100.4 (C-16, C-18), −0.2 ($CH_3$). FT-IR (KBr): $\nu$ = 2959, 2152, 1672, 1593, 1400, 1310, 1242, 1148, 845 cm$^{-1}$. MS (FAB, 3-NOBA): $m/z$ = 373 $[M + H]^+$. Anal. Calcd (%) for $C_{24}H_{24}O_2Si$: C, 77.28; H, 6.49. Found: C, 77.00; H, 6.31.

**1,5-Diethynyl-9,10-anthraquinone (6a), 1,8-Diethynyl-9,10-anthraquinone (6b), and 2,6-Diethynyl-9,10-anthraquinone (6c): General procedure:** The corresponding bis(trimethylsilylethynyl)-9,10-anthraquinone **5a**−**c** (0.2 g, 0.5 mmol) was dissolved in chloroform (10 mL) and heated at reflux. To this mixture a solution of tetrabutylammonium-fluoride (0.42 g, 1.5 mmol) in $CHCl_3$ (5 mL) was added dropwise during 1 h. After 2 h more, water (10 mL) was added and the organic layer was washed with brine and with water. After removal of the solvent, the solid residue was thoroughly washed with methanol and vacuum-dried.

**6a:** Yield: (117 mg, 91%), tan solid. Mp >250 °C. $^1$H NMR (200 MHz, $CDCl_3$, 25 °C, TMS), $\delta$ = 8.38 (dd, $^3J$ = 7.6 Hz, $^4J$ = 1.5 Hz, 2H; H-4, H-8), 7.96 (dd, $^3J$ = 7.6 Hz, $^4J$ = 1.5 Hz, 2H; H-2, H-6), 7.76 (t, $^3J$ = 7.6 Hz, 2H; H-3, H-7), 3.61 (s, 2H; ethynyl). FT-IR (KBr): $\nu$ = 3252, 2098, 1674, 1566, 1431, 1323, 1269, 1161, 1026, 837, 702 cm$^{-1}$. MS (FAB, 3-NOBA): $m/z$ = 257 $[M + H]^+$. Anal. Calcd (%) for $C_{18}H_8O_2$: C, 84.37; H, 3.15. Found: C, 84.13; H, 3.04.

**6b:** Yield: (115 mg, 90%), brown solid with identical physical characteristics to the ones already described.[21]

**6c:** Yield: (110 mg, 86%), light-brown solid. Mp > 250 °C. $^1$H NMR (200 MHz, $CDCl_3$, 25 °C, TMS), $\delta$ = 8.40 (d, $^4J$ = 1.5 Hz, 2H; H-1, H-5), 8.28 (d, $^3J$ = 8.2 Hz, 2H; H-4, H-8), 7.88 (dd, $^3J$ = 8.2 Hz, $^4J$ = 1.5 Hz, 2H; H-3, H-7), 3.38 (s, 2H; ethynyl). FT-IR (KBr): $\nu$ = 3247, 2100, 1671, 1566, 1430, 1321, 1254, 845, 745 cm$^{-1}$. MS (FAB, 3-NOBA): $m/z$ = 257 $[M + H]^+$. Anal. Calcd (%) for $C_{18}H_8O_2$: C, 84.37; H, 3.1. Found: C, 84.09; H, 3.12.

**Acknowledgment.** The authors are grateful for the financial support of the Ministerio de Educación y Ciencia (Spain) and the Comunidad de Madrid through Grants CTQ-2005-08933-BQU and S-0505/PPQ/000225, respectively (T.T.). This work was also partially supported by the U.S. National Science Foundation, Grant CHE-0135786 (L.E.), and the EU (RTN networds "WONDERFULL" and "CASSIUSCLAYS"), Deutsche Forschungsgemeinschaft (SFB 583), and the Office of Basic Energy Sciences of the U.S. Department of Energy (NDRL 4682) (G.L.H. and D.G.).

**Supporting Information Available:** Experimental methods. Selected UV−vis absorption spectra and dilution and pyridine-titration experiments of Pc−AQ−Pc triads **1a**−**c** and Pc **2** in THF, pyridine, *o*-dichlorobenzene, toluene, and benzonitrile. Interpretation of the CV data and OSWVs of **6a**−**c** in THF and of **1a**−**c** and 2 in *o*-DCB. Some selected differential absorption features and time absorption profiles in THF and benzonitrile. This material is available free of charge via the Internet at http://pubs.acs.org.

JA055344+